NO_x-Mediated Homogeneous Pathways for the Synthesis of Formaldehyde from CH_4-O_2 Mixtures

Jeffrey M. Zalc, William H. Green,† and Enrique Iglesia*

Department of Chemical Engineering, University of California at Berkeley, Berkeley, California 94720, and Department of Chemical Engineering, Massachusetts Institute of Technology, Cambridge, Massachusetts 02139

A detailed kinetic network for homogeneous $CH_4-O_2-NO_x$ reactions is used to estimate maximum attainable formaldehyde (and methanol) yields and to identify elementary steps that lead to the observed enhancement effects of NO_x on CH_4 oxidation rates, to HCHO yield limits, and to NO_x losses to unreactive N-compounds. NO_x was shown previously to increase CH_4 oxidation rates and HCHO yields in CH_4-O_2 reactions, but maximum yields were low (<10%) and intrinsic kinetic limits were not rigorously examined. We show here that the CH_4 oxidation rate increases because NO_2 reacts with CH_4 during an initial induction period. NO and NO_2 lead to similar effects, except that residence times required for a given yield are higher for NO feeds because $NO-NO_2$ interconversion must first occur. CH_4 leads to supra-equilibrium NO_2 concentrations because HO_2 formed during HCHO oxidation reacts with NO to form OH and NO_2 faster than NO_2 can decompose to NO. Oxygenate selectivities decrease with increasing CH_4 conversion, because weaker C−H bonds in HCHO and CH_3OH relative to CH_4 lead to their fast sequential oxidation to CO and CO_2. Rate-of-formation analyses show that NO_x molecules introduce more effective elementary steps for the formation of CH_3O intermediates and for its conversion to HCHO, but H-abstraction from CH_4 and HCHO remains the predominant step in controlling rates and selectivities in the presence or absence of NO_x. Without NO_x, OH radicals account for all H-abstraction reactions from CH_4, while HCHO reacts with OH but also with less reactive H and HO_2 radicals. NO_x increases HCHO yields by converting these less reactive H and HO_2 radicals to OH radicals, which become the predominant H-abstractor for both CH_4 and HCHO and which react less selectively with HCHO than do H and HO_2. Kinetic selectivity, based on C−H bond energy differences between CH_4 and HCHO, becomes weaker with increasing radical reactivity and increasing reaction temperature. Maximum HCHO yields of 37% are theoretically possible for radicals that abstract H from CH_4 and HCHO at equal rates, but radical species prevalent during $CH_4-O_2-NO_x$ reactions lead to maximum HCHO yields below 10% under all conditions. Higher yields appear unlikely with more reactive radicals, because their reactivity would lead to cascade reactions that form species with greater kinetic sensitivity to C−H bond energies. Maximum C_1-oxygenate yields increase with increasing O_2 pressure, suggesting that the O_2 distribution along a reactor will not improve HCHO yields but may prove useful to inhibit NO_x losses to less reactive N-compounds.

1. Introduction

The practical conversion of remote natural gas reserves to transportable liquid fuels and chemicals requires multiple steps and synthesis gas intermediates.[1−3] Direct routes may be able to decrease process complexity and capital costs and improve energy efficiency. Oxidative coupling (OCM) to form ethane/ethene[4] is currently impractical because desired C_2 products react further to form CO and CO_2.[5−8] CH_4-O_2 mixtures form HCHO and CH_3OH with low yields (4−7%) on heterogeneous catalysts,[9−14] and homogeneous pathways at high pressures (5−20 MPa O_2) and low temperatures (600−700 K) give only slightly higher yields.[15]

NO added to CH_4-O_2 reactants increased CH_4 conversion rates and C_1-oxygenate yields on V_2O_5/SiO_2 at 850−950 K,[16] as also reported for homogeneous reactions;[17] these homogeneous pathways may avoid undesired HCHO decomposition on even "inert" surfaces.[18−20] Otsuka et al.[21] reported ∼4% C_1-oxygenate yields in homogeneous $NO-CH_4-O_2$ reactions under conditions that did not form detectable products without NO (873 K, 20 kPa CH_4, 10 kPa O_2, 2 kPa NO) and achieved 6.5% HCHO yields after optimization (873 K, 5 kPa CH_4, 2.5 kPa O_2, 0.5 kPa NO).[22] NO is relatively unreactive but forms NO_2 by reaction with O_2, and NO_2 reacts more rapidly with oxygenates than with CH_4,[23] suggesting that direct reactions of NO_2 cannot account for the observed yield enhancements.

Here, we describe a kinetic network for NO_x-mediated homogeneous pathways and explore intrinsic limits on oxygenate yields and routes for NO_x losses to unreactive N-compounds. We use this homogeneous network to probe optimal conditions and process feasibility. The network used builds on $CH_4-O_2-NO_x$ studies addressing NO_x formation during combustion[24−29] by extending GRI-Mech[24] to include oxygenate synthesis in $CH_4-O_2-NO_x$ mixtures and expanding previous studies of NO_x-mediated oxygenate synthesis.[30] In the process, we examine specific steps responsible for the rate and yield enhancements by NO_x.

CH_4 conversion to HCHO and CO_x occurs sequentially via steps influenced by NO_x concentration. H-abstractions from CH_4 and HCHO are the kinetically relevant steps in determining HCHO yields. We find that C−H activation in CH_4 occurs almost exclusively by reactions with OH, but HCHO activation involves H, HO_2, and OH radicals. NO_x increases HCHO yields via chain cycles that convert H and HO_2 to more reactive OH radicals. These OH radicals activate C−H bonds less selectively than H or HO_2 and minimize the kinetic preference for weaker C−H bonds in HCHO. CH_4-O_2-NO mixtures lead to NO_2 levels well above those expected from $NO-O_2$ equilibrium. NO

* To whom correspondence should be addressed. E-mail: iglesia@cchem.berkeley.edu.

† Massachusetts Institute of Technology.

10.1021/ie050885t CCC: $33.50
Published on Web 03/10/2006

Table 1. Comparison of Simulation Results with Experimental Data from Figure 2 (of ref 30) for C-Selectivities for HCHO, CH_3OH, CO, CO_2, and CH_3NO_2 at Several Reaction Temperatures and CH_4 Conversions[a]

		Selectivity (%)									
		HCHO		CH_3OH		CO		CO_2		CH_3NO_2	
T (K)	CH_4 conversion (%)	simulation	data[30]	simulation	data[30]	simulation	data[30]	simulation	data[30]	simulation	data[30]
748	0.7	82.5	57	4.3	12	9.6	14	0.1	2	3.5	*b*
773	3.2	60.5	32	4.8	10	30.1	43	1.0	2	3.5	12
798	7.5	40.0	25	5.1	7	49.1	55	2.3	3	3.4	10
803	10	32.0	22	5.1	6	56.6	60	2.6	3	3.4	9
823	35	1.7	5	0.4	*b*	78.4	77	12.7	9	1.3	1

[a] Data are compared at the same CH_4 conversion, and selectivities are defined on the basis of CH_4 reacted. [b] Data point could not be extracted accurately from Figure 2 in ref 30.

and NO_2 effects on CH_4-O_2 reactions are similar, except for a direct role of NO_2 in chain initiation, which leads to shorter residence times. CH_3NO_2, N_2O, and N_2 form during reaction at residence times required to achieve maximum HCHO yields; these N-losses preclude complete recycling of NO_x in practical processes.

2. Simulation Methods

2.1. Base Mechanism and Modifications. A previous study[30] used GRI-Mech (v. 2.1.1)[24] modified by removing several N-containing species and their reactions and then inserting NO_x, HONO, $HONO_2$, CH_3NO_2, CH_3ONO, CH_2NO_2, CH_3NO, CH_3OO, and CH_3OOH reactions. Here, we use GRI-Mech (v. 3.0) and extend it by adding the reactions in ref 30 not already present in GRI-Mech (v. 3.0). The reaction network contains 65 species and 419 elementary steps. Thermodynamics for species not included in GRI-Mech (v 3.0) were extracted from the CHEMKIN Thermodynamic Database. The full kinetic network and related thermodynamic data are available in CHEMKIN format.[31]

2.2. Reactor Simulations. CHEMKIN 4.0 (Reaction Design, Inc.) was used together with a Fortran code to describe an isothermal and isobaric reactor with plug-flow hydrodynamics. "C_1-oxygenates" denotes the combined HCHO and CH_3OH products. Yield is defined as the percentage of the inlet CH_4 stream that is converted to each product. Peak or maximum yields denote the highest yield attained along a reactor. Selectivities are reported as the CH_4 converted only to HCHO and CO_x (CO and CO_2); they exclude trace C_{2+} products, except for comparisons with experiments (section 3.1), for which all products are reported. Nitrogen selectivities are reported as the percentage of the inlet NO_x appearing as each product. Pathways for formation and conversion of each species were probed using rate-of-formation analysis.[32] A heuristic sequential scheme (section 3.5) was used to interpret simulations; simulations reflect in all cases the complete kinetic network. This simple scheme uses first-order phenomenological rate constants to describe CH_4 to HCHO (k_1) and HCHO to CO_x (k_2) reactions. The ratio k_1/k_2 reflects the relative rates of HCHO synthesis and conversion and influences maximum HCHO yields attainable as CH_4 conversion increases with residence time.

3. Results and Discussion

3.1. Validation of Kinetic Model and Simulations. Table 1 compares simulated HCHO, CH_3OH, CO, CO_2, and CH_3NO_2 selectivities with experimental values at various CH_4 conversions[30] (55.6 kPa CH_4, 27.7 kPa O_2, 0.5 kPa NO) for experiments conducted at constant inlet molar rates and increasing temperature. Simulations were carried out at each temperature, but experimental conversions were matched in the simulations by letting residence times vary. Simulations and data agree relatively well and show the expected decrease in HCHO selectivity with increasing CH_4 conversion; they are also in qualitative agreement with previous reports.[30] This reaction network is used below to probe the mechanistic basis for the effects of NO and NO_2 on CH_4 conversion and C_1-oxygenate yields.

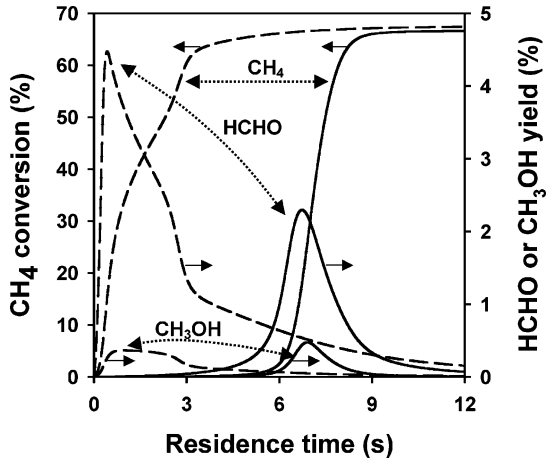

Figure 1. CH_4 conversion and HCHO and CH_3OH yields as a function of reactor residence time at 873 K for reactants with 50 kPa CH_4, 50 kPa O_2, and 0 kPa NO_x (—) or 5 kPa NO (- - -).

3.2. Simulations of NO_x Effects on C_1-Oxygenate Yields. Figure 1 shows that NO (5 kPa) in CH_4-O_2 streams (50 kPa CH_4, 50 kPa O_2) increases maximum C_1-oxygenate yields at 873 K and decreases residence times required for a given CH_4 conversion by shortening the induction periods prevalent in CH_4-O_2 reactions. The maximum C_1-oxygenate yield is 2.7% without NO and is reached at 6.8 s of residence time and 20.3% CH_4 conversion. With 5 kPa NO, the maximum yield is 4.7%; it is reached at 0.4 s and 16.1% CH_4 conversion. NO appears to provide or promote initiation pathways. HCHO and CH_3OH maximum yields occur at similar residence times, and HCHO is the predominant oxygenate formed (~85% without NO; ~94% with 5 kPa NO).

The effects of NO and NO_2 pressures on CH_4-O_2 reactions (50 kPa CH_4, 50 kPa O_2) are shown in Table 2. Maximum C_1-oxygenate yields occur at shorter residence times with NO_2 than with NO. With NO, CH_4 activation can occur via reactions with NO_2, which forms rapidly during reaction. Maximum C_1-oxygenate yields and HCHO/CH_3OH ratios are similar with NO and NO_2. NO_2 and NO have identical kinetic consequences, but NO_2 leads to faster initiation; in fact, product selectivities and CH_4 conversion profiles along the reactor become identical with NO and NO_2 when one of them is shifted by a constant residence time (Table 2).

Molecular simulations[33,34] have shown that NO_2 abstracts H-atoms from CH_4 more effectively than NO or O_2. Activation

Table 2. Peak C_1-oxygenate Yields and Required Residence Times, CH_4 Conversions, and HCHO and CH_3OH Yields at Various NO and NO_2 Inlet Pressures[a]

NO_x pressure (kPa)	peak C_1-oxygenate yield (%)	residence time (s)	CH_4 conversion[b] (%)	HCHO yield[b] (%)	CH_3OH yield[b] (%)
0	2.7	6.8	20.3	2.3	0.5
0.1 (NO)	2.8	4.6	17.8	2.4	0.5
0.1 (NO_2)	2.8	1.1	17.8	2.4	0.5
1 (NO)	4.8	1.4	17.8	4.3	0.5
1 (NO_2)	4.8	0.6	17.4	4.3	0.5
2 (NO)	4.8	0.9	17.5	4.4	0.4
2 (NO_2)	4.8	0.5	17.5	4.4	0.4
5 (NO)	4.7	0.4	16.1	4.5	0.3
5 (NO_2)	4.6	0.3	18.1	4.3	0.3

[a] Conditions: 873 K, 50 kPa CH_4, 50 kPa O_2, no diluent. [b] At the residence time leading to the peak C_1-oxygenate yield.

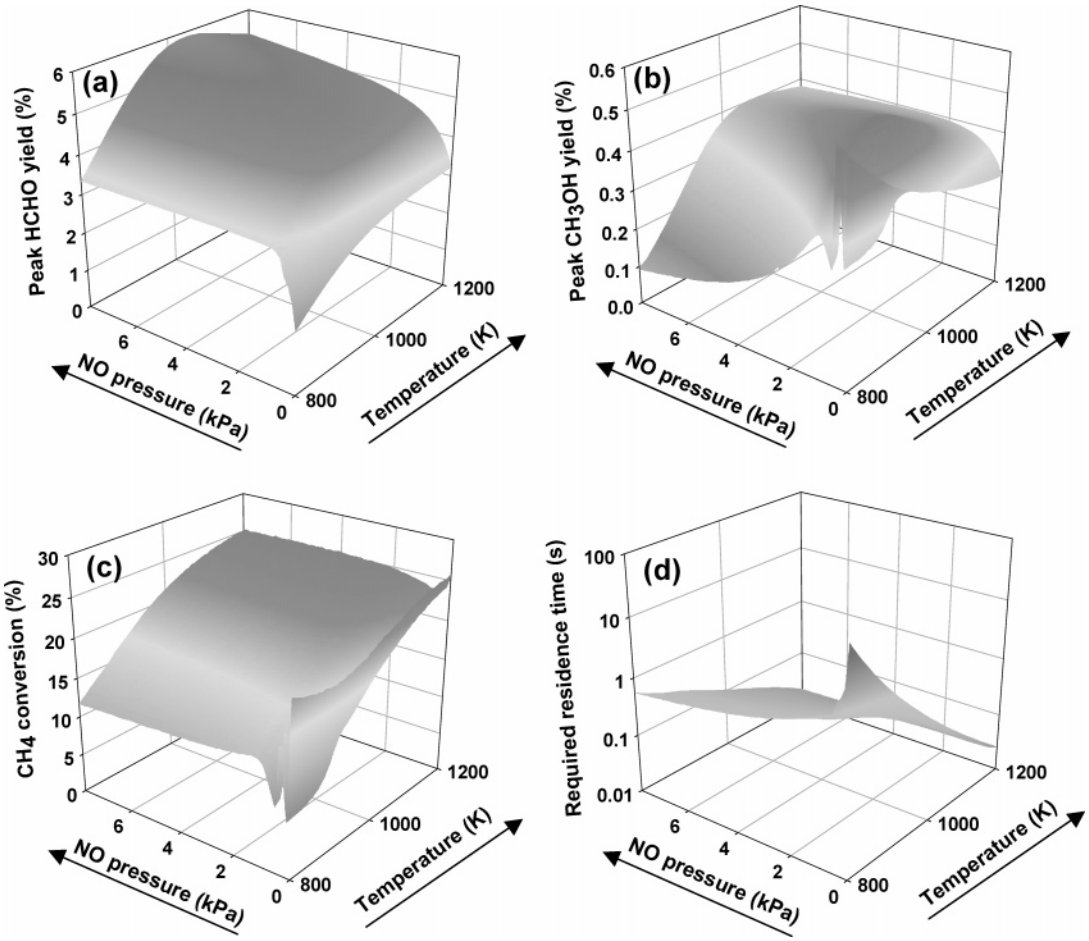

Figure 2. HCHO yields (a), CH_3OH yields (b), CH_4 conversions (c), and required reactor residence times (d) as a function of reaction temperature and inlet NO pressure. All data are shown for residence times leading to the peak total C_1-oxygenate yield at each temperature and NO pressure (50 kPa CH_4, 50 kPa O_2, no diluent).

barriers were 65.6 and 37.6 kcal/mol for NO and NO_2, respectively, and 59.0 kcal/mol for O_2. At ambient pressure and 873 K[22] or 1200 K,[35] CH_4−NO mixtures did not react, as also found in our simulations for equimolar NO−CH_4 mixtures at 873 K and up to 5 ks of residence time. Simulations with NO_2−CH_4 mixtures, however, showed 35% CH_4 conversion at 1.6 s with 70, 19, 8, and 11% selectivities to CO_2, CO, HCHO, and CH_3NO_2. The differences between CH_4−O_2−NO and CH_4−O_2−NO_2 merely reflect the time required to form NO_2 in the case of CH_4−O_2−NO mixtures (section 3.9).

Predicted maximum C_1-oxygenate yields and the residence times required to achieve them are shown in Figure 2 at 800−1200 K and 0−8 kPa inlet NO pressure (50 kPa CH_4, 50 kPa O_2). Maximum HCHO yields increased with temperature, because stronger C−H bonds in CH_4 require higher activation energies than weaker C−H bonds in HCHO (or CH_3OH). HCHO yields increased with increasing NO pressure. Experiments at 873 K and ambient pressure with 5.0 kPa CH_4, 2.5 kPa O_2, and 0.5 kPa NO gave a HCHO/CH_3OH ratio of 32,[22] while simulations predict a value of 38 at these conditions. Peak oxygenate yields occur at intermediate CH_4 conversions (10−25%; Figure 2c), because HCHO converts to CO_x in sequential reactions as residence time increases. Residence times required for maximum C_1-oxygenate yields decreased with increasing temperature and NO pressure (Figure 2d).

The observed decrease in HCHO yields with increasing residence time (Figure 1) resembles that for homogeneous and catalytic CH_4−O_2 reactions[20,23,36,37] (e.g., oxidative coupling[5,8,38]). Prevalent secondary reactions reflect the more reactive nature of the desired products (HCHO, C_2H_4, C_2H_6) compared with CH_4 reactants. HCHO and CO_x selectivities are shown in Figure 3 at 873 K as a function of the CH_4 conversion

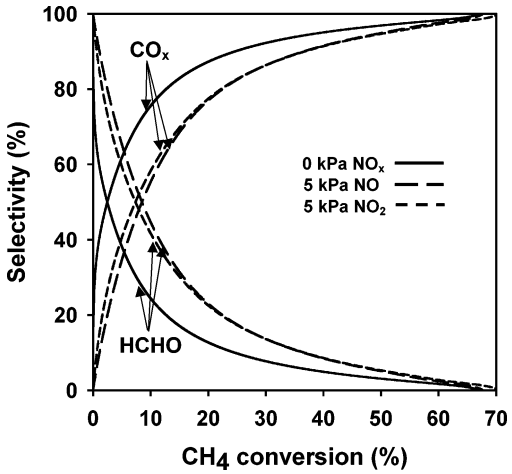

Figure 3. HCHO and CO_x selectivities as a function of CH_4 conversion for reactants with 0 kPa NO_x (—), 5 kPa NO (— — —), or 5 kPa NO_2 (- - -). Selectivities are based only on the HCHO and CO_x products formed (873 K, 50 kPa CH_4, 50 kPa O_2, no diluent).

and residence time for CH_4-O_2 mixtures (50 kPa CH_4, 50 kPa O_2) and NO_x pressures of 0 and 5 kPa. HCHO selectivities are ~100% when extrapolated to zero CH_4 conversion. NO and NO_2 increase HCHO yields by inhibiting selectivity losses caused by secondary reactions.

3.3. Pathways for HCHO Synthesis and Consumption with and without NO_x. Next, we discuss the effects of NO_x on specific elementary steps involved in HCHO synthesis and oxidation. Rate-of-formation analysis can be used to identify species and steps responsible for HCHO formation and conversion and the influence of NO_x on such steps. The evolution of the most abundant carbon-containing radicals and of all stable molecules proceeds via

$$CH_4 \rightarrow CH_3 \rightarrow CH_3O \rightarrow HCHO \rightarrow HCO \rightarrow CO \rightarrow CO_2 \quad (1)$$

with CH_3NO_2, formed via reactions of CH_3 with NO_2, and CH_3OH, formed from CH_3O, as minor side reactions. H-addition to CH_3O from H_2 or CH_4 forms more than 90% of all CH_3OH molecules. The sequential nature of the reactions in eq 1 has been proposed for CH_4-O_2 and $CH_4-O_2-NO_x$ reactants,[27,29,36,39] but detailed contributions and the relative kinetic relevance of the various elementary steps involved remain unclear.

Figures 4 and 5 show rate-of-formation data for CH_4 and HCHO, respectively, including steps that form or convert >2% of all CH_4 and HCHO. Without NO_x, CH_4-O_2 reactions proceed mostly (>90%) via H-abstraction from CH_4 using OH radicals (Figure 4a):

$$OH + CH_4 = CH_3 + H_2O \quad (2)$$

with small contributions from H-abstraction by H radicals. With NO (5 kPa NO; Figure 4b), H-abstraction by OH also accounts for >90% of the CH_4 converted; abstraction by NO_2 (formed from NO) is involved in ~4% of CH_4 conversion events:

$$NO_2 + CH_4 = CH_3 + HONO \quad (3)$$

Reaction 3, however, provides an efficient route for activating C−H bonds during the initial induction period,[40−42] consistent with the shorter induction observed when NO_2 is used instead of NO; NO forms NO_2 during CH_4-O_2-NO reactions only after a finite residence time. Two maxima in CH_4 conversion rates

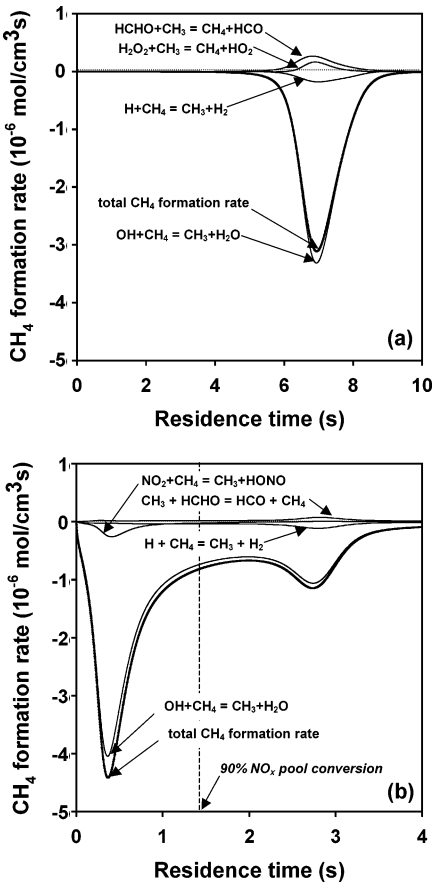

Figure 4. Rate-of-formation analysis for CH_4 for reactants with 0 kPa NO_x (a) or 5 kPa NO (b) (873 K, 50 kPa CH_4, 50 kPa O_2, no diluent).

occur with NO (5 kPa NO; at ~0.4 s and ~2.7 s); the latter one reflects CH_3O dissociation to HCHO and H, as NO_x is depleted with increasing residence time.

The elementary steps that convert CH_3 to CH_3O depend on the NO_x concentration. Without NO_x, CH_3O forms predominantly (>99%) via

$$HO_2 + CH_3 = CH_3O + OH \quad (4)$$

which converts HO_2 into reactive OH radicals; OH abstracts H-atoms from CH_4 about 10^5 times faster than HO_2 (at 873 K). With NO (5 kPa), most of the HO_2 forms OH by reacting with NO, reaction (20), a step that accounts for ~80% of the OH formed. With the resulting low $[HO_2]$ and high $[NO_2]$, ~97% of the CH_3O is formed by reaction (5):

$$NO_2 + CH_3 = CH_3O + NO \quad (5)$$

Simulations of NO_x abatement by reburning suggest that CH_3O forms via NO_2-CH_3 reactions at 750−1250 K;[27] these steps involve NO_2 formed via $NO-NO_2$ interconversion in CH_4-O_2 mixtures (section 3.9). Thus, the elementary steps responsible for CH_3 conversion to CH_3O depend on NO_x concentrations, as discussed in section 3.4.

HCHO formation rates are shown in Figure 5 at 873 K for equimolar CH_4-O_2 mixtures with 0 kPa (a) and 5 kPa (b) NO. Without NO, HCHO forms predominantly via

$$CH_3O = HCHO + H \quad (6)$$

$$O_2 + CH_3O = HCHO + HO_2 \quad (7)$$

These steps account for 95% of the HCHO molecules formed.

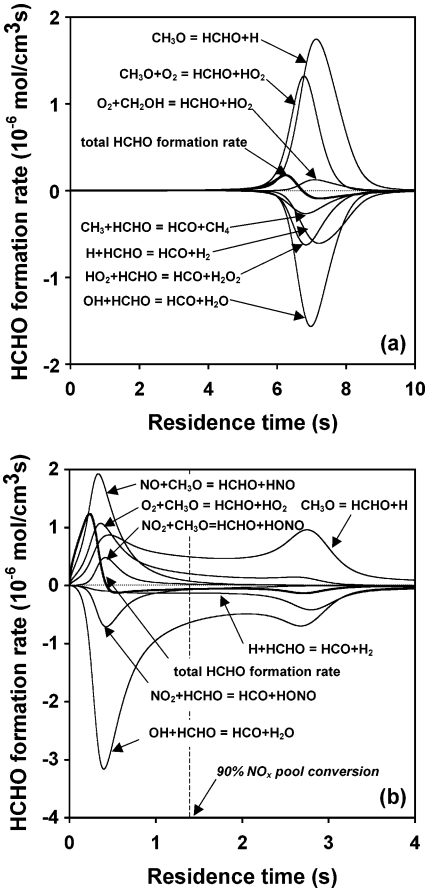

Figure 5. Rate-of-formation analysis for HCHO for reactants with 0 kPa NO_x (a) or 5 kPa NO (b) (873 K, 50 kPa CH_4, 50 kPa O_2, no diluent).

NO (5 kPa) introduces two other routes for CH_3O conversion to HCHO (Figure 5b):

$$NO + CH_3O = HCHO + HNO \quad (8)$$

$$NO_2 + CH_3O = HCHO + HONO \quad (9)$$

which account for 22% and 5%, respectively, of all HCHO formed. Tabata et al.[17,34] suggested that NO_x provides faster routes for CH_3O conversion to HCHO. Figure 5b shows that after most NO_x and O_2 molecules are converted, CH_3O dissociation forms H radicals (at ~2.7 s of residence time); H radicals then convert directly to OH via reactions with NO_2 or combine with O_2 to form HO_2, which, in turn, forms OH by reactions with NO. These paths to OH radicals lead to the increase in CH_4 conversion rates shown in Figure 4b.

HCHO is the desired intermediate within sequential CH_4 oxidation reactions that ultimately form CO and CO_2. Thus, strategies for increasing HCHO yields require that we also understand HCHO oxidation pathways. Without NO_x (Figure 5a), HCHO is consumed predominantly via

$$OH + HCHO = HCO + H_2O \quad (10)$$

$$H + HCHO = HCO + H_2 \quad (11)$$

$$HO_2 + HCHO = HCO + H_2O_2 \quad (12)$$

which account for 46, 24, and 19% of all the HCHO consumed. With 5 kPa NO (Figure 5b), reactions 10−12 account for 68, 19, and 2%, indicating that NO_x increases HCHO yields by converting H and HO_2 to OH radicals, which react less selectively with HCHO (vs CH_4) than H or HO_2. Figure 5b also shows that

$$NO_2 + HCHO = HCO + HONO \quad (13)$$

accounts for 15% of all the HCHO consumed. NO_2, however, also introduces other HCHO conversion routes. HCHO formation rates up to the residence times required for maximum C_1-oxygenate yields (Figure 5a; 0 kPa NO_x) indicate that reactions 10−12 account for 43, 13, and 27% of HCHO consumption. With NO (5 kPa; Figure 5b), 82, 3, 0.1, and 15% of HCHO conversion occurs via reactions 10−13, respectively. NO_x increases HCHO yields by inhibiting HCHO reactions, through a shift in the radical pool to OH at the expense of H and HO_2 radicals, which are much less effective in activating the C−H bonds in CH_4 than those in HCHO.

This rate-of-formation analysis can identify relevant synthesis and destruction pathways for HCHO in CH_4−O_2 and CH_4−O_2−NO_x mixtures, but it cannot quantify HCHO yield enhancements with NO_x in terms of specific kinetically-relevant steps or of rate constants for simpler reaction sequences. We describe next sensitivity analysis methods to identify those steps with the strongest influence on maximum HCHO yields.

3.4. Sensitivity of Peak HCHO Yields to Rate Constants of Elementary Steps. The sensitivity of maximum HCHO yields [$Y_{HCHO}(\tau_{peak})$] to the rate constant for the ith elementary step, k_i, is[43]

$$S_i = \frac{d(\ln(Y_{HCHO}(\tau_{peak})))}{d(\ln(k_i))} \quad (14)$$

S_i is the (fractional) change in the maximum HCHO yield for a given (fractional) change in k_i. Positive values indicate that maximum HCHO yields increase with increasing k_i. A k_i change of 0.1 was used to estimate S_i. We note that residence times for maximum HCHO yields, τ_{peak}, vary slightly as rate constants are perturbed.

Figure 6 shows the 10 elementary steps with the greatest value of S_i (at 873 K, 50 kPa CH_4, 50 kPa O_2) with 0 kPa (a) or 5 kPa (b) NO. Without NO_x, maximum HCHO yields depend most sensitively on H-abstraction from CH_4 and HCHO by OH. CH_3−HO_2 reactions to form CH_3O and OH (reaction 4) also have positive effects on HCHO yields. Figure 6a shows negative S_i values for H-abstraction from HCHO, specifically by H (reaction 11) and HO_2 (reaction 12). Termination steps, such as HO_2 recombination to form H_2O_2 and O_2 or CH_3 recombination to give C_2H_6, also decrease maximum HCHO yields. With 5 kPa NO (Figure 6b), the highest S_i values were also for H-abstraction from CH_4 and HCHO by OH radicals, showing that NO_x-assisted rates for CH_3 conversion to CH_3O and for CH_3O conversion to HCHO do not introduce detectable kinetic bottlenecks.

3.5. Kinetic Basis for HCHO Yield Improvements by NO_x. CH_4 conversion to HCHO and then to CO_x occurs via a complex reaction network, which can be described qualitatively by

$$CH_4 \xrightarrow{k_1} HCHO \xrightarrow{k_2} CO_x \quad (15)$$

where k_1 and k_2 are phenomenological pseudo-first-order rate constants for the CH_4 to HCHO and HCHO to CO_x conversions, respectively. These k_1 and k_2 rate constants reflect complex contributions from intervening radicals, whose concentrations and kinetic contributions vary as the reaction proceeds and as NO_x concentrations change along a reactor. The ratio of these

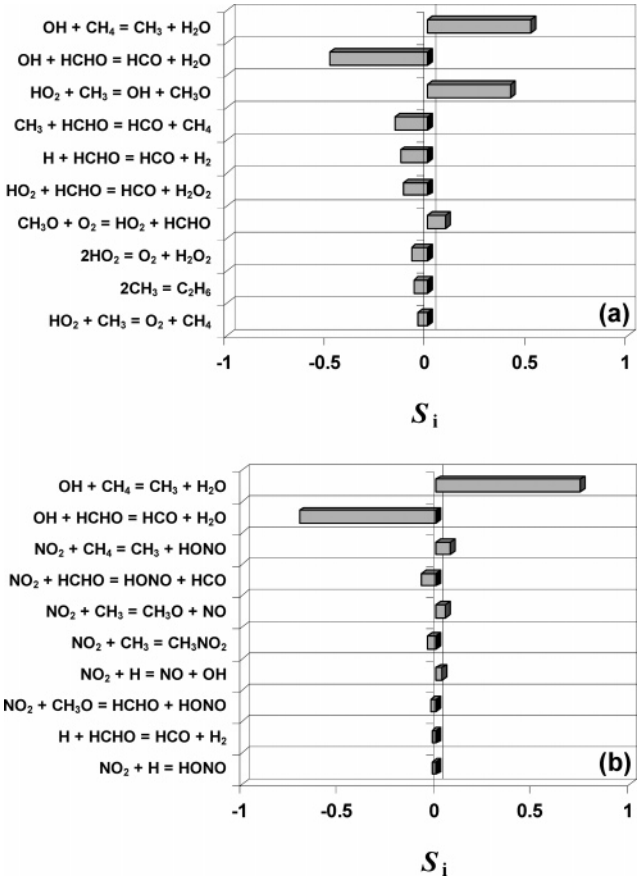

Figure 6. Sensitivity analysis results showing elementary steps whose rate constants most strongly influence peak HCHO yields for reactants with 0 kPa NO_x (a) or 5 kPa NO (b). As defined in eq 14, S_i is the fractional change in the peak HCHO yield relative to the fractional change in the rate constant of elementary step i (873 K, 50 kPa CH_4, 50 kPa O_2, no diluent).

rate constants (k_1/k_2) determines the maximum attainable HCHO yields. Mole balances for CH_4 and HCHO based on the reaction sequence in eq 15 give the local ratio of these pseudoconstants:

$$\frac{k_2}{k_1} = \left(\frac{\mathrm{d}(\ln[\mathrm{HCHO}])}{\mathrm{d}(\ln[\mathrm{CH_4}])} + \frac{[\mathrm{CH_4}]}{[\mathrm{HCHO}]} \right) \tag{16}$$

from our simulations and allow us to examine the effects of NO and NO_2 concentrations on this ratio. Values of k_1 can be obtained from CH_4 conversion and the partial pressure at each residence time:

$$k_1 = -\frac{1}{[\mathrm{CH_4}]} \frac{\mathrm{d}[\mathrm{CH_4}]}{\mathrm{d}t} = -\frac{\mathrm{d}(\ln[\mathrm{CH_4}])}{\mathrm{d}t} \tag{17}$$

HCHO yields, k_1/k_2 ratios, and k_1 values are shown as a function of CH_4 conversion in Figure 7 for CH_4-O_2, CH_4-O_2-NO, and $CH_4-O_2-NO_2$ mixtures at 873 K. The k_1/k_2 ratios (Figure 7a) are higher when NO_x is present, consistent with the higher maximum HCHO yields achieved when NO_x is present in the inlet stream (Figure 7b). The k_1/k_2 ratios increase with increasing CH_4 conversion, because radical intermediates increase in concentration and form HCHO; ultimately, radical concentrations decrease because O_2 depletion influences HCHO formation more strongly than its conversion. For CH_4 conversions below 25%, NO_x increases the pseudo-first-order rate constants for CH_4 conversion (Figure 7c) and k_1 values are greater for NO_2 than for NO. NO and NO_2 show similar effects on k_1/k_2 ratios (Figure 7a) and HCHO yields (Figure 7b), but NO_2 shortens induction periods more effectively than NO.

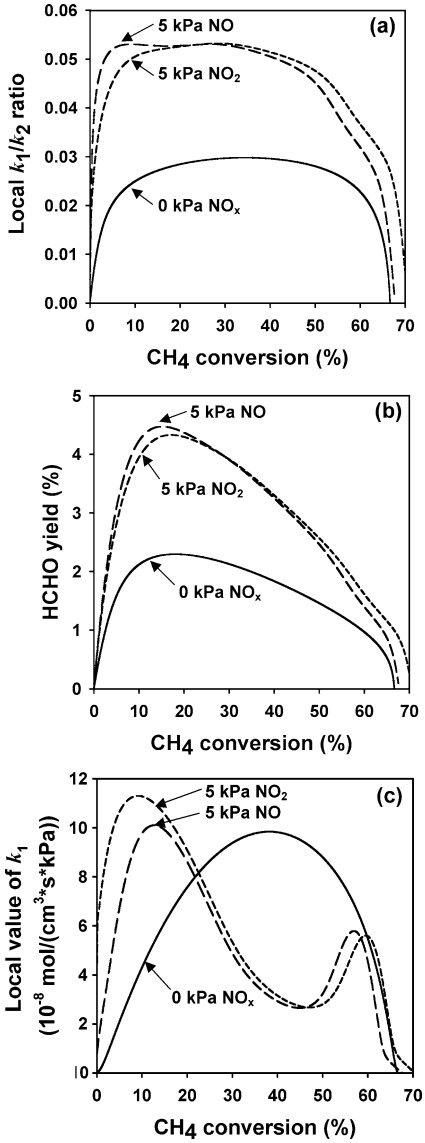

Figure 7. Simulation results for local k_1/k_2 values (a), HCHO yields (b), and k_1 (c) as a function of CH_4 conversion for reactants with 0 kPa NO_x (—), 5 kPa NO (− − −), or 5 kPa NO_2 (- - -) (873 K, 50 kPa CH_4, 50 kPa O_2, no diluent).

Maximum HCHO yields reflect k_1/k_2 ratios, while k_1 depends mostly on OH levels, because reaction 2 accounts for most CH_4 activation events (except ~4% from H-abstraction by NO_2). Values of k_2 depend on radical concentrations, and H-abstraction reactions by OH, H, HO_2, and NO_2 (reactions 10−13) all contribute to HCHO depletion. Thus, k_1/k_2 is given by

$$\frac{k_1}{k_2} \approx \frac{k_{\mathrm{CH_4}}^{\mathrm{OH}}[\mathrm{OH}]}{k_{\mathrm{HCHO}}^{\mathrm{OH}}[\mathrm{OH}] + k_{\mathrm{HCHO}}^{\mathrm{H}}[\mathrm{H}] + k_{\mathrm{HCHO}}^{\mathrm{HO_2}}[\mathrm{HO_2}] + k_{\mathrm{HCHO}}^{\mathrm{NO_2}}[\mathrm{NO_2}]} \tag{18}$$

where k_j^R is the rate constant for H-abstraction from j by species R. Equation 18 can be written as

$$\frac{k_1}{k_2} \approx \frac{k_{\mathrm{CH_4}}^{\mathrm{OH}}}{k_{\mathrm{HCHO}}^{\mathrm{OH}}} \left[1 + \frac{k_{\mathrm{HCHO}}^{\mathrm{H}}}{k_{\mathrm{HCHO}}^{\mathrm{OH}}} \frac{[\mathrm{H}]}{[\mathrm{OH}]} + \frac{k_{\mathrm{HCHO}}^{\mathrm{HO_2}}}{k_{\mathrm{HCHO}}^{\mathrm{OH}}} \frac{[\mathrm{HO_2}]}{[\mathrm{OH}]} + \frac{k_{\mathrm{HCHO}}^{\mathrm{NO_2}}}{k_{\mathrm{HCHO}}^{\mathrm{OH}}} \frac{[\mathrm{NO_2}]}{[\mathrm{OH}]} \right]^{-1} \tag{19}$$

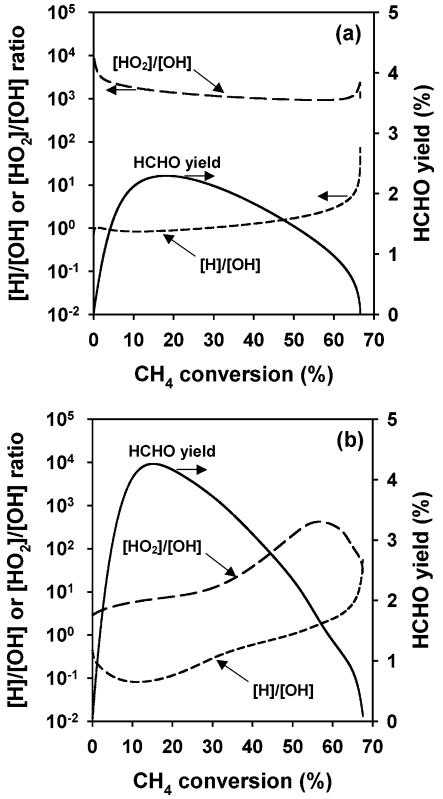

Figure 8. HO_2/OH (− −) and H/OH (- - -) ratios (left vertical axis) and HCHO yield (—) (right vertical axis) as functions of CH_4 conversion for reactants with 0 kPa NO_x (a) or 5 kPa NO (b) (873 K, 50 kPa CH_4, 50 kPa O_2, no diluent).

where $k^{H}_{HCHO}/k^{OH}_{HCHO}$, $k^{HO_2}_{HCHO}/k^{OH}_{HCHO}$, and $k^{NO_2}_{HCHO}/k^{OH}_{HCHO}$ are 4×10^{-1}, 3×10^{-4}, and 2×10^{-6}, respectively, at 873 K (from rate constants in our kinetic network). These k_1/k_2 ratios increase as [H]/[OH], [HO_2]/[OH], and [NO_2]/[OH] ratios decrease; their highest value is $k^{OH}_{CH_4}/k^{OH}_{HCHO} = 0.06$ at 873 K. Thus, high HCHO yields require NO_x, which decreases [H]/[OH] and [HO_2]/[OH] ratios by increasing OH concentrations at the expense of H and HO_2 concentrations.

3.6. Effect of Nitrogen Oxides on the Composition of the Pool of Radical Intermediates. Figure 8 shows [H]/[OH] and [HO_2]/[OH] ratios and HCHO yields as a function of CH_4 conversion for 0 kPa NO_x (a) and 5 kPa NO (b) at 873 K. NO_x markedly decreases [H]/[OH] and [HO_2]/[OH] ratios, because it is involved in conversion of H and HO_2 to OH. At maximum HCHO yields, [HO_2]/[OH] is ∼1400 without NO_x (Figure 8a), but it is only ∼7 with 5 kPa NO (Figure 8b). [H]/[OH] ratios are ∼0.9 and ∼0.1 for 0 and 5 kPa NO, respectively.

Without NO_x, ∼60% of OH radicals form via HO_2 reactions with CH_3 (reaction 4) and ∼30% form via H_2O_2 dissociation. With 5 kPa NO, the latter contributes only 2%, while NO_x-mediated OH generation cycles,

$$HO_2 + NO = NO_2 + OH \tag{20}$$

$$NO_2 + H = NO + OH \tag{21}$$

form ∼81 and ∼14% of all OH radicals, respectively, and 98% of all HO_2 formed is converted to OH via reaction 20, instead of participating in H-abstraction from HCHO. Reactions 20−21 provide pathways for converting H and HO_2 radicals to OH,[29,44] thereby decreasing the rate of destruction of HCHO via selective reactions of these radicals with HCHO.

3.7. Radical Reactivity and Intrinsic Limitations on Maximum HCHO Yields. The highest k_1/k_2 values in eq 19 are achieved when reactive contributions by [H], [HO_2], and [NO_2] become insignificant; then, k_1/k_2 ratios reflect solely the relative reactivity of OH radicals in abstracting H-atoms from CH_4 and HCHO ($k^{OH}_{CH_4}/k^{OH}_{HCHO} = 0.06$ at 873 K). Figure 9 shows the maximum HCHO yield for the scheme in eq 15 as a function of the k_1/k_2 ratio. A rate constant ratio of 0.06 leads to a maximum HCHO yield of 5.3%, while a value of 37% is expected for unselective H-abstraction from CH_4 or HCHO (i.e., $k_1/k_2 = 1$). At 5 kPa NO (at 873 K), our simulations give maximum HCHO yields of 4.5%, similar to those found for H-abstraction by OH radicals. C_1-oxygenate yields reach asymptotic values with increasing NO_x pressure (Figure 2a), because H and HO_2 are fully converted to OH and they are no longer involved in destructive reactions that abstract H from HCHO.

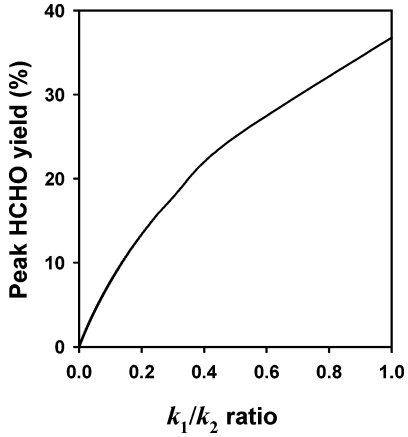

Figure 9. Peak HCHO yield attainable as a function of the k_1/k_2 ratio for the consecutive reaction scheme given by eq 15.

Species that abstract H-atoms from HCHO less selectively than OH would lead to even higher HCHO yields. Batiot and Hodnett[23] proposed that maximum yields in oxidation reactions are related to differences in energy between the weakest C−H bond in reactants and products. Large C−H energy differences (>30 kJ/mol) lead to yield losses via rapid secondary reactions. C−H bond energies in CH_4 and HCHO are 439 kJ/mol and 369 kJ/mol,[45] respectively, consistent with the low HCHO yields predicted (Figure 2) and measured.[9,12,13,16,18,20−22,36,46] This proposal is consistent with the results in Figure 10, where $k^{R}_{CH_4}/k^{R}_{HCHO}$ ratios are shown to depend on the enthalpy of the R + H = R−H reaction, where R is a H-abstractor. The $k^{R}_{CH_4}/k^{R}_{HCHO}$ ratios are lower than unity and increase as R + H = R−H reactions become more exothermic; they approach unity only at very large R−H bond energies, when reactions of R become insensitive to differences in C−H bond energies. For OH, the $k^{R}_{CH_4}/k^{R}_{HCHO}$ ratio is 0.06 at 873 K and the enthalpy for OH + H = HO−H reactions is −507 kJ/mol. More reactive H-abstractors should, in principle, be even less selective and lead to higher C_1-oxygenate yields, but their concentrations are likely to be quite low as a result of their reactivity and of their involvement in cascade reactions that form radicals selective for HCHO activation. These arguments also account for an increase in maximum HCHO yields with increasing temperature (Figure 2a), because the selectivity of H-abstraction reactions decreases as all radicals react faster with increasing temperature.

3.8. Mechanism for NO_x Losses During Reactions of CH_4−O_2−NO_x Mixtures. In CH_4−O_2−NO_x mixtures, NO_x forms less reactive N-compounds at residence times required to reach maximum HCHO yields (Figure 11a). CH_3NO_2 forms at low temperatures (<873 K, 20 kPa CH_4, 10 kPa O_2, 2 kPa NO).[21,22]

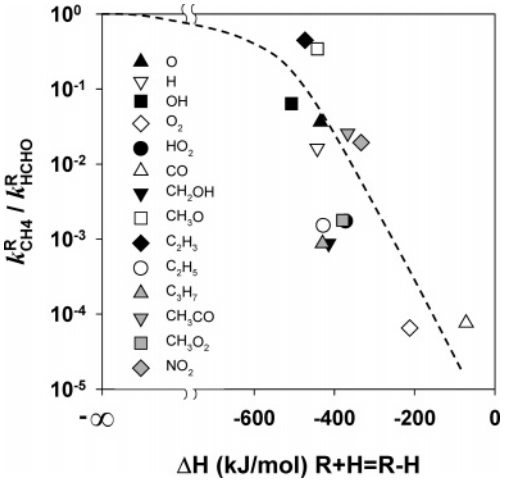

Figure 10. At 873 K, ratio of rate constants $k^R_{CH_4}/k^R_{HCHO}$ for H-abstraction from CH_4 relative to HCHO for various abstracting entities, R, plotted as a function of the ΔH for the recombination reaction R + H = R−H. The rate constants are expected to be comparable only if both reactions are extremely exothermic, as suggested by the dotted line.

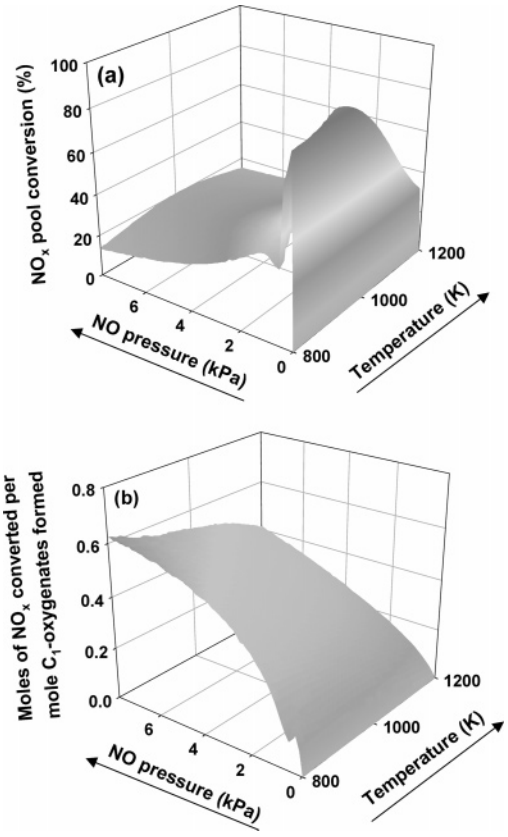

Figure 11. NO_x pool conversions (a) and moles of NO_x converted per mole of C_1-oxygenates formed (b) as functions of reaction temperature and inlet NO at residence times leading to maximum oxygenate yields (50 kPa CH_4, 50 kPa O_2, no diluent).

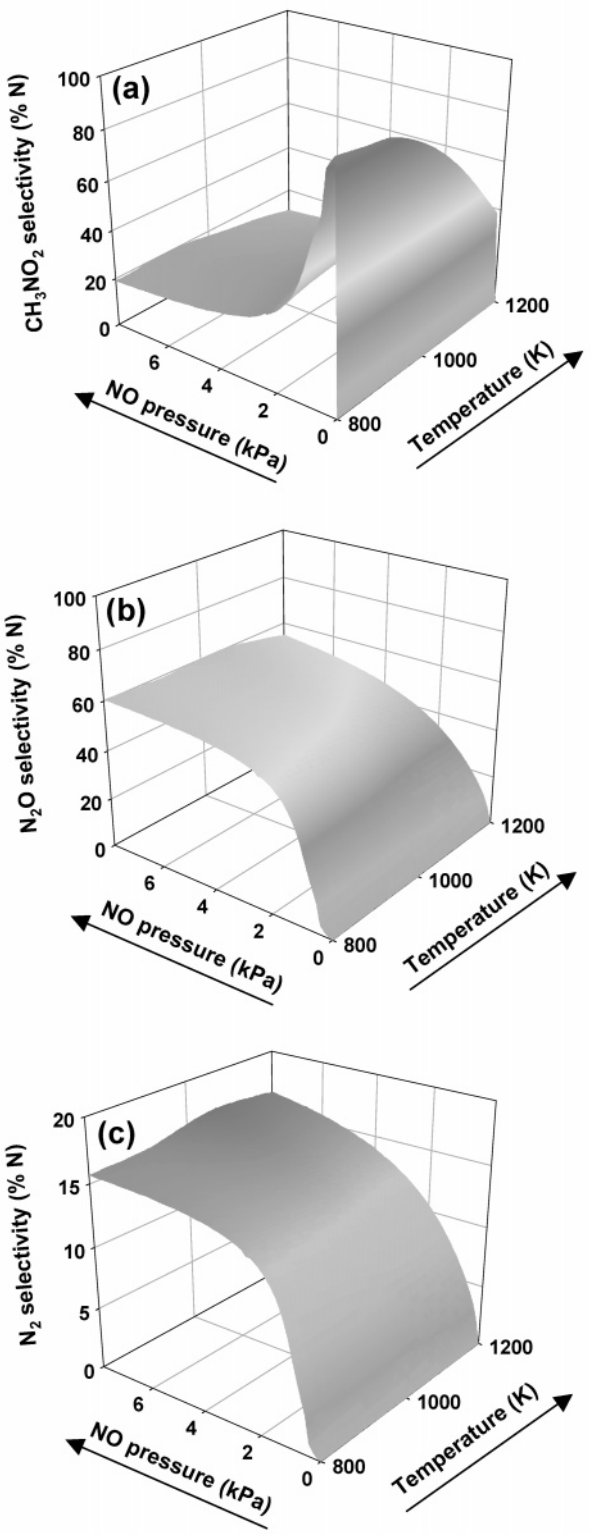

Figure 12. Nitrogen selectivities for CH_3NO_2 (a), N_2O (b), and N_2 (c) as functions of reaction temperature and inlet NO pressure at residence times leading to the peak C_1-oxygenate yield (50 kPa CH_4, 50 kPa O_2, no diluent).

Teng et al.[47] reported ∼10% selectivity to CH_3NO_2 (on a carbon basis) at 10% CH_4 conversion and complete NO_x conversion. Yan et al.,[48] however, failed to detect CH_3NO_2 by infrared measurements of effluent streams. $CH_4-O_2-NO_2$ mixtures led to 40−80% NO_2 conversion at 673−733 K with CH_3NO_2 as the main product.[49]

NO_x pool conversion initially decreased with increasing NO pressure but, then, remained at ∼13−15% at 800−1200 K as pressure increased (Figure 11a). The ratio of NO_x consumed per C_1-oxygenate formed at maximum HCHO yield increased with NO pressure (Figure 11b). Figure 12 shows N-selectivities for CH_3NO_2 (a), N_2O (b), and N_2 (c) at maximum C_1-oxygenate yields and various temperatures and NO pressures. CH_3NO_2 selectivities increased with NO pressure (up to ∼0.2 kPa NO) but N_2O became the predominant product at higher NO pressures. At 2 MPa total pressure, CH_3NO_2 selectivities were slightly higher but the observed trends resemble those shown

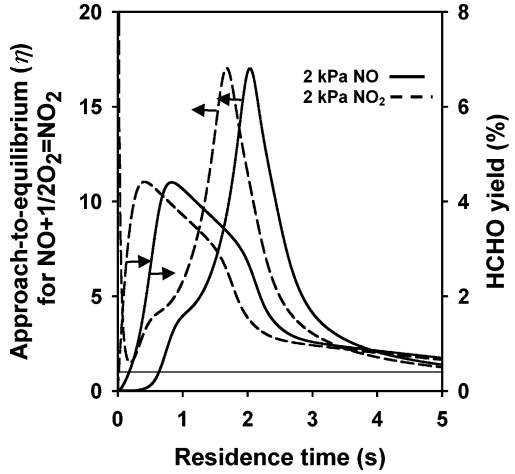

Figure 13. Approach-to-equilibrium, η, (eq 26) for NO + $^1/_2O_2$ = NO_2 (left vertical axis) and HCHO yield (right vertical axis) as functions of residence time for reactants with 2 kPa NO (—) or 2 kPa NO_2 (- - -) (873 K, 50 kPa CH_4, 50 kPa O_2, no diluent).

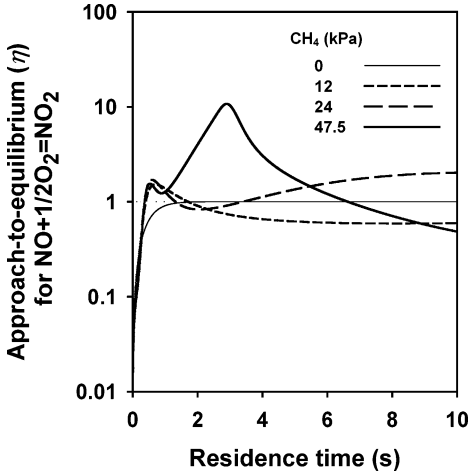

Figure 14. Approach-to-equilibrium, η, (eq 26) for NO + $^1/_2O_2$ = NO_2 as a function of reactor residence time for reactants with 0, 12, 24, or 47.5 kPa CH_4 (873 K, 100 kPa total, 5 kPa NO, 47.5 kPa O_2, balance Ar).

in Figure 11 at ambient pressure. Rate-of-formation analysis showed that CH_3NO_2, N_2O, and N_2 form predominantly via

$$NO_2 + CH_3 = CH_3NO_2 \quad (22)$$

$$NH + NO = N_2O + H \quad (23)$$

$$NH + NO = N_2 + OH \quad (24)$$

NH forms predominantly (97%) by HNO reactions with CO, and reactions 23 and 24 consume 96% of all NH formed. These simulations show that NO_x converts to less reactive molecules during CH_4-O_2 reactions via mechanisms resembling those that cause the observed effects of NO_x on HCHO yields; thus, decoupling desired and undesired homogeneous reactions of NO_x is unlikely and on-purpose synthesis of replacement NO_x seems inevitable in practice.

3.9. Supra-equilibrium NO_2 Concentrations by Addition of CH_4 to $NO-O_2$ Mixtures. The approach to equilibrium (η) for direct conversion of NO to NO_2

$$NO + {}^1/_2O_2 = NO_2 \quad (25)$$

is given by

$$\eta = \frac{1}{K_{eq}} \frac{P_{NO_2}}{P_{NO}\sqrt{P_{O_2}}} \quad (26)$$

where K_{eq} is the equilibrium constant for reaction 25 (0.325 $atm^{-1/2}$ at 873 K) and η becomes unity at equilibrium. Otsuka et al.[21] measured η values for $NO-NO_2$ conversion at 773 K using infrared spectroscopy and concluded that $NO-O_2$ and NO_2-O_2 equilibrations require much longer residence times (40−80 times) than maximum HCHO yields with CH_4-O_2-NO reactants; they also concluded that $NO-NO_2$ did not equilibrate during CH_4-O_2-NO reactions.

Our results show instead that CH_4 increases $NO-NO_2$ equilibration rates and forms NO_2 at levels above those for $NO-O_2$ equilibrium (eq 25) at residence times required for maximum HCHO yields. Figure 13 shows η values and HCHO yields for CH_4-O_2-NO and $CH_4-O_2-NO_2$ reactants as a function of residence time. With NO, η is initially zero and reaches unity at ~0.6 s and a maximum value (~17) at longer residence times. The η value is 2.9 when maximum HCHO yields are reached. With NO_2, η starts at very high values, but the curves are otherwise similar, except that they are shifted, together with HCHO yields, to shorter residence times. Curiously, a reductant (CH_4) increases the rate of formation of oxidized molecules (NO_2).

Next, we probe these effects by replacing CH_4 with Ar in $NO-O_2$ mixtures. With $NO-O_2-Ar$, η increases monotonically toward unity (Figure 14; 0.99 at 1.7 s), but it exceeds unity as inlet CH_4 pressures increase. Previous studies reported an increase in NO oxidation rates by CH_4 in the context of homogeneous combustion processes.[44] NO_2 accounts for 40% (experiments) and 55% (simulations) of NO_x species for streams with 50 ppm CH_4 and 20 ppm NO in ambient air at 1000 K;[44] these NO_2 levels correspond to η values of 12−23. Our simulations under these conditions also gave high η values. These supra-equilibrium NO_2 concentrations reflect kinetic coupling of elementary steps and not thermodynamic inconsistencies in the reaction network.

Figure 13 shows that increases in η occur slightly after increases in HCHO yields along the reactor; η values rise sharply as maximum HCHO yields are reached, suggesting a mechanistic connection between the HCHO and NO_2 formation pathways. NO_2-CH_3 reactions to form CH_3O and NO (reaction 5) consume 70% of the NO_2 formed and produce 97% of all the CH_3O formed (at 873 K, 5 kPa NO, 50 kPa CH_4, 50 kPa O_2). HCHO forms HCO via the sequence in eq 1, with 96% of all HCO consumed by reaction with O_2:

$$HCO + O_2 = HO_2 + CO \quad (27)$$

HO_2 forms as HCO is consumed in reaction 27 and then reacts with NO to give OH and NO_2 (eq 20), which forms NO_2 faster than NO_2 can decompose to reestablish $NO-O_2$ equilibrium. The sequence of transformations in eq 1 accounts for supra-equilibrium NO_2 levels and for the higher OH concentrations and HCHO yields when NO_x is added to CH_4-O_2 mixtures.

3.10. Effect of CH_4 and O_2 Partial Pressures on Oxygenate Yields. Figure 15a shows maximum C_1-oxygenate yields obtained at 873 K without NO_x over a wide range of CH_4 and O_2 pressures (0.1−50 MPa CH_4 and O_2). These maximum yields depend slightly on the total pressure for equimolar reactants (2.5−3% for 0.02−10 MPa). The HCHO fraction in the oxygenates increases with total pressures (84% at 0.1 MPa; 54% at 10 MPa), as also found experimentally.[15,50,51] Maximum oxygenate yields are limited by O_2 depletion at low O_2/CH_4

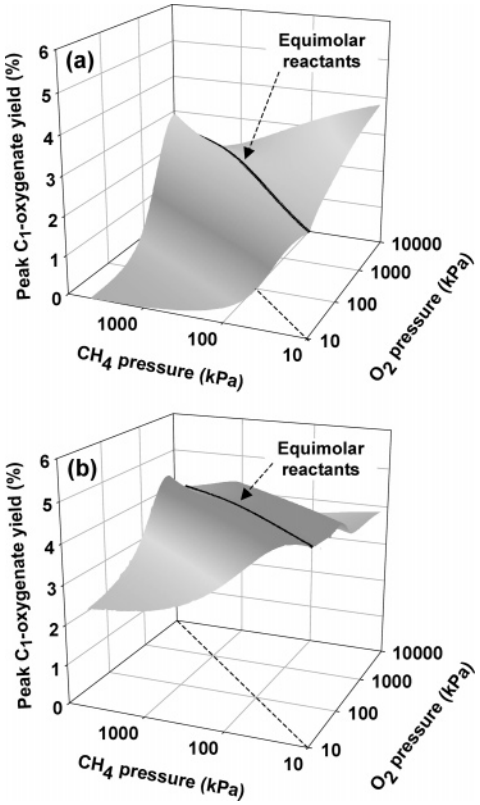

Figure 15. Peak C_1-oxygenate yield as a function of inlet CH_4 and O_2 pressures at 873 K without NO_x (a) and for a ratio of NO_2 to CH_4 inlet pressures equal to 0.1 (b). Solid lines are drawn to show equal CH_4 and O_2 inlet pressures.

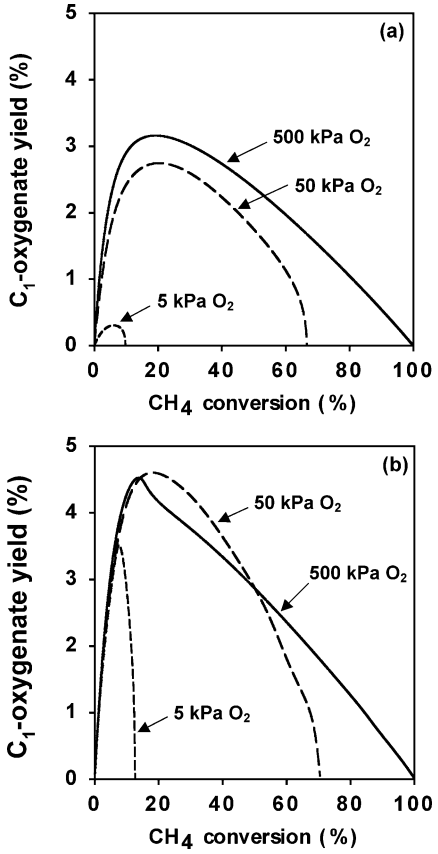

Figure 16. C_1-oxygenate yield as a function of CH_4 conversion at several inlet O_2 pressures, 50 kPa CH_4, and 0 kPa NO_x (a) or 5 kPa NO_2 (b) (873 K).

ratios. Figure 15b shows maximum C_1-oxygenate yields at NO_2/CH_4 inlet ratios of 0.1 for similar ranges of CH_4 and O_2 pressures. NO_2 increases these yields for all inlet CH_4 and O_2 pressures. The O_2 depletion effects on maximum yields are weaker than those without NO_2, because NO_2 acts as an additional stoichiometric source of oxygen atoms.

If O_2 pressure influences the relative rates of HCHO formation and consumption, staged O_2 feeds can be used to satisfy stoichiometric O_2 requirements while minimizing O_2 pressures along the reactor. C_1-oxygenate yields are shown as a function of CH_4 conversion for inlet O_2 pressures of 5, 50, and 500 kPa and inlet streams with 50 kPa CH_4 without NO_x (Figure 16a) and with 5 kPa NO_2 (b). In both cases, yields increased with increasing inlet O_2 pressure, suggesting that O_2 increases HCHO formation rates more strongly than HCHO consumption rates. With 5 kPa NO_2, maximum oxygenate yields are 3.3, 4.3, and 4.5% for feeds with 5, 50, and 500 kPa O_2. Figure 15 shows that the highest oxygenates yields are attained for nearly equimolar CH_4-O_2 mixtures during CH_4 oxidation to HCHO mediated by NO_x. Thus, distributed O_2 addition along a reactor is unlikely to increase C_1-oxygenate yields, but it may prove useful in maintaining low local NO_x pressures and minimizing the formation of unreactive CH_3NO_2, N_2O, and N_2.

4. Conclusions

We have assembled a detailed kinetic mechanism for reactions of $CH_4-O_2-NO_x$ mixtures and confirmed that addition of NO or NO_2 to CH_4-O_2 reactants decreases residence times required for CH_4 conversion and enhances C_1-oxygenate yields (HCHO $\gg$ CH_3OH). Required residence times for CH_4 conversion and oxygenate formation are greater for NO than NO_2, which is able to activate C−H bonds in CH_4 and is generated during reaction when NO_x is fed as NO. Peak oxygenate yields are essentially identical with NO and NO_2 and increase both with reaction temperature and with NO_x pressure. Rate-of-formation analyses show that CH_4 conversion to HCHO and CO_x occurs sequentially, with NO_x modifying pathways available for the transformations. We probed the sensitivity of the maximum HCHO yield to rate constants of individual elementary steps and found that H-abstractions from CH_4 and from HCHO are the most kinetically significant. OH radicals account for virtually all H-abstraction from CH_4, while conversion of HCHO involves H, HO_2, OH, and NO_2. In the absence of NO_x, conversion of HO_2 to OH via reaction with CH_3 is also kinetically relevant and is a major production route for OH. Nitrogen oxides allow the rapid conversion of less reactive H and HO_2 radicals to OH, which reacts less selectively with HCHO (relative to CH_4).

We used a heuristic consecutive reaction scheme with pseudo-first-order rate constants to describe the conversion of CH_4 and formation of HCHO and CO_x products, and we showed that NO_x changes the ratio of rate constants responsible for maximum HCHO yields by reducing the [H]/[OH] and [HO_2]/[OH] ratios. Even if less reactive H and HO_2 radicals were completely converted to OH, HCHO yields would be limited by OH selectivity in activating the weaker C−H bond in HCHO than that in CH_4. We showed that the presence of an even more energetic radical than OH could lead to improved yield performance, although the maximum theoretical single-pass yield of 37% would only be attained using an infinitely energetic radical that is unable to distinguish the difference in C−H bond strengths in HCHO and CH_4. Independently varying the CH_4 and O_2 pressures between 10 and 5000 kPa suggested that the highest oxygenate yields are obtained for nearly equimolar CH_4-O_2 mixtures and that increasing the total pressure has a

minimal effect on the maximum oxygenate yields. Increasing O_2 pressure enhances the elementary steps leading to C_1-oxygenate formation more than those involved in the sequential reactions of these oxygenates. The use of staged introduction of either O_2 or CH_4 along a reactor will not lead to improved yields of C_1-oxygenates, which appear intrinsically limited to $<10\%$ during reactions of $CH_4-O_2-NO_x$ mixtures.

At residence times leading to the maximum oxygenate yields, significant conversion of NO and NO_2 to CH_3NO_2, N_2O, and N_2 occurs, thereby wasting the NO_x "catalyst" and leading to increased residence time requirements. Formation of CH_3NO_2 is a termination step acting as a sink for CH_3 radicals and NO_2 molecules, while formation of N_2O and N_2 results from reaction of NO with NH. Although distributed CH_4 or O_2 addition would not improve oxygenate yields, staged NO_x introduction might minimize NO_x losses to unreactive N-compounds. We also found strong kinetic limitations in the nitrogen chemistry that lead to NO_2 concentrations far above those expected from the equilibrium of $NO + {}^1/_2O_2 = NO_2$. This interesting behavior shows that the presence of a reductant (CH_4) increases the concentration of oxidized molecules (NO_2).

Acknowledgment

This study was supported by BP as part of the Methane Conversion Cooperative Research Program at the University of California at Berkeley. The technical guidance and support of Dr. Theo Fleisch are acknowledged with thanks.

Literature Cited

(1) Aasberg-Petersen, K.; Hansen, J.-H. B.; Christensen, T. S.; Dybkjaer, I.; Christensen, P. S.; Nielsen, C. S.; Madsen, S. E. L. W.; Rostrup-Nielsen, J. R. Technologies for large-scale gas conversion. *Appl. Catal., A* **2001**, *221*, 379.

(2) Reyes, S. C.; Sinfelt, J. H.; Feeley, J. S. Evolution of processes for synthesis gas production: Recent advances in an old technology. *Ind. Eng. Chem. Res.* **2003**, *42*, 1588.

(3) Rostrup-Nielsen, J. R. Production of synthesis gas. *Catal. Today* **1993**, *18*, 305.

(4) Keller, G. E.; Bhasin, M. M. Synthesis of ethylene via oxidative coupling of methane. I. Determination of active catalysts. *J. Catal.* **1982**, *73*, 9.

(5) Labinger, J. A.; Ott, K. C. Mechanistic studies on the oxidative coupling of methane. *J. Phys. Chem.* **1987**, *91*, 2682.

(6) Su, Y. S.; Ying, J. Y.; Green, W. H. Upper bound on the yield for oxidative coupling of methane. *J. Catal.* **2003**, *218*, 321.

(7) Mleczko, L.; Baerns, M. Catalytic oxidative coupling of methane—reaction engineering aspects and process schemes. *Fuel Process. Technol.* **1995**, *42*, 217.

(8) Androulakis, I. P.; Reyes, S. C. Role of distributed oxygen addition and product removal in the oxidative coupling of methane. *AIChE J.* **1999**, *45*, 860.

(9) Spencer, N. D.; Pereira, C. J. Partial oxidation of CH_4 to HCHO over a MoO_3-SiO_2 catalyst: A kinetic study. *AIChE J.* **1987**, *33*, 1808.

(10) Spencer, N. D.; Pereira, C. J. V_2O_5-SiO_2-catalyzed methane partial oxidation with molecular oxygen. *J. Catal.* **1989**, *116*, 399.

(11) Parmaliana, A.; Arena, F. Working mechanism of oxide catalysts in the partial oxidation of methane to formaldehyde: Catalytic behaviour of SiO_2, MoO_3/SiO_2, TiO_2, and V_2O_5/TiO_2 systems. *J. Catal.* **1997**, *167*, 57.

(12) Hall, T. J.; Hargreaves, J. S. J.; Hutchings, G. J.; Joyner, R. W.; Taylor, S. H. Catalytic synthesis of methanol and formaldehyde by partial oxidation of methane. *Fuel Process. Technol.* **1995**, *42*, 151.

(13) Arena, F.; Parmaliana, A. Scientific basis for process and catalyst design in the selective oxidation of methane to formaldehyde. *Acc. Chem. Res.* **2003**, *36*, 867.

(14) Zhang, X.; He, D.; Zhang, Q.; Ye, Q.; Xu, B.; Zhu, Q. Selective oxidation of methane to formaldehyde over Mo/ZrO_2 catalysts. *Appl. Catal., A* **2003**, *249*, 107.

(15) Hunter, N. R.; Gesser, H. D.; Morton, L. A.; Yarlagadda, P. S.; Fung, D. P. C. Methanol formation at high pressure by the catalyzed oxidation of natural gas and by the sensitized oxidation of methane. *Appl. Catal.* **1990**, *57*, 45.

(16) Bañares, M. A.; Cardoso, J. H.; Hutchings, G. J.; Bueno, J. M. C.; Garcia-Fierro, J. L. Selective oxidation of methane to methanol and formaldehyde over V_2O_5/SiO_2 catalysts. Role of NO in the gas phase. *Catal. Lett.* **1998**, *56*, 149.

(17) Tabata, K.; Teng, Y.; Takemoto, T.; Suzuki, E.; Bañares, M. A.; Peña, M. A.; Garcia-Fierro, J. L. Activation of methane by oxygen and nitrogen oxides. *Catal. Rev.—Sci. Eng.* **2002**, *44*, 1.

(18) Irusta, S.; Lombardo, E. A.; Miró, E. E. Effects of NO and solids on the oxidation of methane to formaldehyde. *Catal. Lett.* **1994**, *29*, 339.

(19) Baldwin, T. R.; Burch, R.; Squire, G. D.; Tsang, S. C. Influence of homogeneous gas-phase reactions in the partial oxidation of methane to methanol and formaldehyde in the presence of oxide catalysts. *Appl. Catal.* **1991**, *74*, 137.

(20) Foulds, G. A.; Gray, B. F. Homogeneous gas-phase partial oxidation of methane to methanol and formaldehyde. *Fuel Process. Technol.* **1995**, *42*, 129.

(21) Otsuka, K.; Takahashi, R.; Yamanaka, I. Oxygenates from light alkanes catalyzed by NO_x in the gas phase. *J. Catal.* **1999**, *185*, 182.

(22) Otsuka, K.; Takahashi, R.; Amakawa, K.; Yamanaka, I. Partial oxidation of light alkanes by NO_x in the gas phase. *Catal. Today* **1998**, *45*, 23.

(23) Batiot, C.; Hodnett, B. K. The role of reactant and product bond energies in determining limitations to selective catalytic oxidations. *Appl. Catal., A* **1996**, *137*, 179.

(24) http://www.me.berkeley.edu/gri_mech/.

(25) Glarborg, P.; Alzueta, M. U.; Dam-Johansen, K.; Miller, J. A. Kinetic modeling of hydrocarbon/nitric oxide interactions in a flow reactor. *Combust. Flame* **1998**, *115*, 1.

(26) Glarborg, P.; Alzueta, M. U.; Kjaergaard, K.; Dam-Johansen, K. Oxidation of formaldehyde and its interaction with nitric oxide in a flow reactor. *Combust. Flame* **2003**, *132*, 629.

(27) Bendtsen, A. B.; Glarborg, P.; Dam-Johansen, K. Low-temperature oxidation of methane: The influence of nitrogen oxides. *Combust. Sci. Technol.* **2000**, *151*, 31.

(28) Hughes, K. J.; Tomlin, A. S.; Hampartsoumian, E.; Nimmo, W.; Zsély, I. G.; Ujvári, M.; Turányi, T.; Clague, A. R.; Pilling, M. J. An investigation of important gas-phase reactions of nitrogenous species from the simulation of experimental measurements in combustion systems. *Combust. Flame* **2001**, *124*, 573.

(29) Loeffler, G.; Wargadalam, V. J.; Winter, F.; Hofbauer, H. Chemical kinetic modelling of the effect of NO on the oxidation of CH_4 under fluidized bed combustor conditions. *Fuel* **2002**, *81*, 855.

(30) Takemoto, T.; Tabata, K.; Teng, Y.; Yao, S.; Nakayama, A.; Suzuki, E. Optimization of C_1-oxygenates for the selective oxidation of methane in a gas-phase reaction of CH_4-O_2-NO at atmospheric pressure. *Energy Fuels* **2001**, *15*, 44.

(31) http://iglesia.cchem.berkeley.edu/mechanism.html.

(32) Bendtsen, A. B.; Glarborg, P.; Dam-Johansen, K. Visualization methods in analysis of detailed chemical kinetics modelling. *Comput. Chem.* **2001**, *25*, 161.

(33) Yamaguchi, Y.; Teng, Y.; Shimomura, S.; Tabata, K.; Suzuki, E. Ab initio study for selective oxidation of methane with NO_x ($x = 1,2$). *J. Phys. Chem. A* **1999**, *103*, 8272.

(34) Tabata, K.; Teng, Y.; Yamaguchi, Y.; Sakurai, H.; Suzuki, E. Experimental verification of theoretically calculated transition barriers of the reactions in a gaseous selective oxidation of $CH_4-O_2-NO_2$. *J. Phys. Chem. A* **2000**, *104*, 2648.

(35) Yan, Z.; Xiao, C.-X.; Kou, Y. NO_x-catalyzed gas-phase activation of methane: A reaction study. *Catal. Lett.* **2003**, *85*, 129.

(36) Pitchai, R.; Klier, K. Partial oxidation of methane. *Catal. Rev.—Sci. Eng.* **1986**, *28*, 13.

(37) Herman, R. G.; Sun, Q.; Shi, C.; Klier, K.; Wang, C.-B.; Hu, H.; Wachs, I. E.; Bhasin, M. M. Development of active oxide catalysts for the direct oxidation of methane to formaldehyde. *Catal. Today* **1997**, *37*, 1.

(38) Reyes, S. C.; Iglesia, E.; Kelkar, C. P. Kinetic-transport models of bimodal reaction sequences—I. Homogeneous and heterogeneous pathways in oxidative coupling of methane. *Chem. Eng. Sci.* **1993**, *48*, 2643.

(39) Lissianski, V. V.; Zamansky, V. M.; Gardiner, W. C. Combustion Chemistry Modeling. In *Gas-Phase Combustion Chemistry*; Gardiner, W. C., Ed.; Springer: New York, 2000.

(40) Slutskii, V. G. Effect of nitrogenous promoters on the low-temperature ignition lag of methane mixtures. *Combust. Explos. Shock Waves* **1985**, *21*, 138.

(41) Slack, M. W.; Grillo, A. R. Shock-tube investigation of methane-oxygen ignition sensitized by NO_2. *Combust. Flame* **1981**, *40*, 155.

(42) Chan, W. T.; Heck, S. M.; Pritchard, H. O. Reaction of nitrogen dioxide with hydrocarbons and its influence on spontaneous ignition. *Phys. Chem. Chem. Phys.* **2001**, *3*, 56.

(43) Varma, A.; Morbidelli, M.; Wu, H. *Parametric Sensitivity in Chemical Systems*; Cambridge University Press: Cambridge, 1999.

(44) Faravelli, T.; Frassoldati, A.; Ranzi, E. Kinetic modeling of the interactions between NO and hydrocarbons in the oxidation of hydrocarbons at low temperatures. *Combust. Flame* **2003**, *132*, 188.

(45) Blanksby, S. J.; Ellison, G. B. Bond dissociation energies of organic molecules. *Acc. Chem. Res.* **2003**, *36*, 255.

(46) Parmaliana, A.; Arena, F.; Sokolovskii, V.; Frusteri, F.; Giordano, N. A comparative study of the partial oxidation of methane to formaldehyde on bulk and silica supported MoO_3 and V_2O_5 catalysts. *Catal. Today* **1996**, *28*, 363.

(47) Teng, Y.; Sakurai, H.; Tabata, K.; Suzuki, E. Methanol formation from methane partial oxidation in CH_4-O_2-NO gaseous phase at atmospheric pressure. *Appl. Catal., A* **2000**, *190*, 283.

(48) Yan, Z.; Xiao, C.-X.; Kou, Y. NO_x-catalyzed gas-phase activation of methane: *In situ* IR and mechanistic studies. *Catal. Lett.* **2003**, *85*, 135.

(49) Han, L.-B.; Tsubota, S.; Haruta, M. Effect of the addition of nitrogen dioxide on the gas-phase partial oxidation of methane with oxygen under normal pressures. *Chem. Lett.* **1995**, *10*, 931.

(50) Gesser, H. D.; Hunter, N. R. The Direct Conversion of Methane to Methanol by Controlled Oxidation. *Chem. Rev.* **1985**, *85*, 235.

(51) Yarlagadda, P. S.; Morton, L. A.; Hunter, N. R.; Gesser, H. D. Direct conversion of methane to methanol in a flow reactor. *Ind. Eng. Chem. Res.* **1988**, *27*, 252.

Received for review July 28, 2005
Revised manuscript received December 11, 2005
Accepted January 27, 2006

IE050885T